Journal of Modern Researches on Electronic Defense Systems

Receive: 24 December 2024 Accept: 31 January 2025

Metamaterial Antenna with Butler Matrix and Wideband Phase Control

Asghar Bakhtiari[2]*
Corresponding Author: asghar.bakhtiari@iau.ac.ir

1. Department of Engineering, Takestan Branch, Islamic Azad University, Takestan, Iran.

Abstract – *This paper introduces a novel, compact broadband beam steering array antenna leveraging a Butler matrix feed network. Addressing the challenges of short-range mm-wave propagation, we propose a dual-pronged approach: broadside single-antenna elements and a Butler matrix-based feed network. The single elements, compact zeroth-order resonance antennas, are efficiently fed via the aperture technique. To further enhance performance, we explore the integration of metamaterial mushroom structures, enabling low-distance operation and reduced mutual coupling. The proposed 16-element (4x4) array, with 0.35λ inter-element spacing, achieves a broadband impedance bandwidth of 32-38 GHz and a wide scan angle of approximately 93°. This innovative design aims to deliver a high-gain, broadside beam steering antenna. The paper presents a detailed, step-by-step process, including simulations and measurements, to realize this novel antenna mushroom structures, enabling low-distance operation and reduced mutual coupling. These structures can effectively manipulate electromagnetic waves, minimizing signal interference between adjacent antenna elements. The proposed 16-element (4x4) array, with 0.35λ inter-element spacing, achieves a broadband impedance bandwidth of 32-38 GHz and a wide scan angle of approximately 93°. This innovative design aims to deliver a high-gain, broadside beam steering antenna, crucial for applications requiring precise beam directionality and efficient signal transmission in the mm-wave band. The paper presents a detailed, step-by-step process, including simulations and measurements, to realize this novel antenna. This comprehensive approach encompasses the design, optimization, and characterization of the antenna array, providing valuable insights into its performance and potential applications.*

Keywords: *Metamaterials, Beam steering, Array Antenna, Butler Matrix.*

1. Introduction

Millimeter-wave (mm-wave) systems have emerged as a promising solution for future telecommunication networks due to their ability to provide high data rates and access less-congested frequency spectrums. These systems are particularly advantageous for compact devices and applications requiring substantial bandwidth. However, designing antennas for mm-wave applications presents significant challenges, such as high atmospheric attenuation that limits communication range. To address this, beam-steering antennas have been proposed as a viable solution, enabling directional radiation patterns to mitigate propagation losses and enhance link reliability [1–9]. Beam-steering antennas generally consist of two key components: feed networks and radiating elements. The radiating elements must exhibit wide beamwidth to maintain stable data transmission irrespective of user positions, making them ideal for point-to-multipoint and short-range applications like indoor Wireless Personal Area Networks (WPANs) [6–8]. One approach to achieve this involves using high-dielectric substrates to reduce antenna size; however, this typically results in narrower bandwidth and lower radiation efficiency. To overcome these limitations, Butler matrix feed networks have gained traction due to their low-loss characteristics and capability to efficiently steer beams over wide angles [10–13]. Despite these advantages, the development of Butler matrix networks at mm-wave frequencies has received limited attention. Previous studies, such as [8], demonstrated a 60 GHz Butler matrix with a

bandwidth of 3 GHz, using RT/Duroid 5880 substrate (dielectric constant 2.2, thickness 0.127 mm). The antenna achieved gains between 7 and 8.9 dBi but relied on patch or quasi-Yagi configurations in linear arrays. Other efforts, including [9], presented 2×4 and 4×4 slot antenna arrays integrated with Butler matrices. These systems demonstrated impedance bandwidths of approximately 0.8 GHz and 0.7 GHz, respectively, with gains ranging from 5 to 7 dBi. In this work, a novel mm-wave beam-steering antenna is introduced, addressing the limitations of previous designs. The proposed system integrates a 4×4 Butler matrix with 16 radiating elements optimized for minimal mutual coupling and stable performance. By employing a compact aperture-coupled hybrid antenna, combining zeroth-order resonance (ZOR) mode with TM010_{010}010 mode, the design achieves a wide beamwidth and high gain [1–3]. The inter-element spacing is set to 0.35λ\lambdaλ, effectively reducing electromagnetic interactions between elements. Comparative analysis with simple patch antennas demonstrates that this configuration significantly lowers mutual coupling. Additionally, the Butler matrix is enhanced with a modified broadband 45° phase shifter, addressing issues like crossovers and phase-shifting limitations that typically increase network size and complexity. The resulting design delivers a stable broadside pattern at 35 GHz, supporting high-efficiency beam steering. This paper provides a comprehensive discussion of the design methodology, simulations, and experimental validations, highlighting the advantages of the proposed approach.

2. Design Procedure

Figure 1 illustrates the geometry of the proposed single antenna, which is constructed using two substrates separated by a ground with an aperture. The top substrate is RT/Duroid 5880, with a relative permittivity of, a loss tangent of, and a thickness of. This layer contains the radiating elements. The bottom substrate, Rogers 3010, houses the microstrip feed line. The radiating elements consist of a mushroom antenna and a parasitic ring patch, generating a TM mode for a directional radiation pattern and a ZOR mode for an omnidirectional pattern. These modes are synthesized to achieve a wide E-plane half-power beamwidth (HPBW). The equivalent circuit of the antenna is shown in Figure 2 [1, 2]. It includes components for the aperture, parasitic ring patch antenna, and mushroom antenna. Coupling coefficients represent interactions between the aperture, mushroom, and parasitic patch. The extracted equivalent parameters are:
where is the vacuum permeability, is the average strip length, and is the patch width?
The input impedance of the slot is calculated as described in [11]. The mutual inductance between the microstrip patch and parasitic patch is:

where is the effective parasitic patch length? Using Agilent ADS optimization, the values for the equivalent circuit are finalized. Simulated results, presented in Figure 3(a), show resonance at 34.9 GHz. The E-plane HPBW and peak gain are 138° and 7.21 dBi, respectively [2].It comprises an aperture (C1, Ca, La, and Ra), a parasitic ring patch antenna (Cp, Lp, and Rp), and a mushroom antenna (CR, LL, and Rm). Γm, Γp, and Γpm are the coupling coefficients between an aperture and a mushroom, an aperture and a parasitic ring patch, and a mushroom and a patch respectively. The equivalent elements of the antenna are extracted as follows: C1=8.82 fF, Ca=139.54 fF, La=160.99 nH, Ra=2295 X, Cp=52.61 pF, Lp=765.08 nH, Rp=905 X, CR=92.22 pF, LL=206.01 nH, Rm=778 X, Γm=0.132, Γp=0.123, and Γpm=0.085 The first step is to model the mushroom with an RLC (resistor-inductor-capacitor) network. The formulas to represent a resonator as a parallel resonant circuit can be found in [1–4] and [10], when the resonator is coupled to the excitation source. The equivalent sheet inductance, LL, and the equivalent sheet capacitance, CR, are given in [10]. The properties of the characteristic parasitic patch can be obtained by using:

$$L_P = \frac{\frac{\mu_0}{2} l_{avg}}{4}\left[Ln\left(\frac{l_{avg}}{w}\right) - 2\right] \quad (1)$$

where μ0 is the vacuum permeability and lavg is the average strip length calculated over all the rings.
The second step is to find the input impedance of the slot, which is calculated by the method suggested in [11]. As is well known, the impedance of a microstrip is as follows. Where Zc is the characteristic impedance of the transmission line and R is the voltage reflection coefficient; and Wa, La and h are the slot width, the slot length, and the substrate height respectively; and the mutual inductance between the microstrip patch and parasitic patch is:

$$M = \frac{\mu_0 x_1}{2\pi}\left[0.467 + \frac{0.059w^2}{x_1^2}\right] \quad (2)$$

where w is the patch width (Wp) and x1 is the effective parasitic patch length. Finally, by optimizing results by Agilent ADS, the values of the equivalent circuit are attained. Figure 3(a) shows the simulated S11 of the antenna. The simulated frequency resonance occurs at 34.9 GHz. The simulated E-plane HPBW and peak gain are 138° and 7.21 dBi [2]. Among the advantages of the proposed antenna elements, compared with a simple patch at 0.35λ0 antenna, is the low mutual coupling between them. Fig. 3 illustrates the comparison between the proposed antenna with the simulated mutual coupling and a simple patch in the 0.35λ0 distance. Clearly, this structure with more than about 15dB lower coupling of elements is superior to the simple patch.

The optimal dimensions of the antenna are as follows: Wp=2 mm, Wh=1.3 mm, radius of the via Vr=0.1 mm, La=2 mm, Wa=0.1 mm, h1=0.508 mm, h2=0.25 mm, Lstub=1 mm. The parameters were found from full wave simulation (ANSYS HFSS). The size of the patch antenna (Wp) and that of the etched hole (Wh) are determined to set the resonance frequency at 35 GHz, and the size of the aperture (La) and radius of via (Vr) are set to optimize the radiation efficiency of the mushroom antenna [2]. A comparison of the proposed antenna's simulated mutual coupling with a simple patch antenna at 0.35 separation is shown in Figure 3. The proposed design achieves approximately 15 dB lower mutual coupling. Optimized dimensions for the antenna are: The size of the patch antenna and the etched hole are chosen to set the resonance frequency at 35 GHz. Aperture size and via radius are optimized to maximize radiation efficiency of the mushroom antenna [2]. Simulated and the radiation pattern at 35 GHz are shown in Figure 4. For further details, refer to [2].

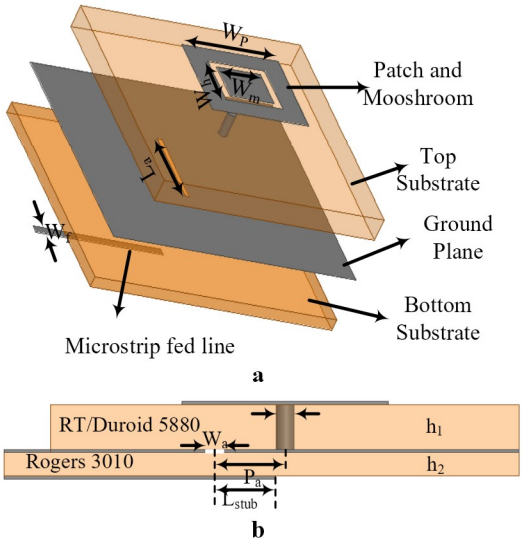

Figure 1. Configuration of proposed ZOR antenna element. a) perspective view, and b) side view

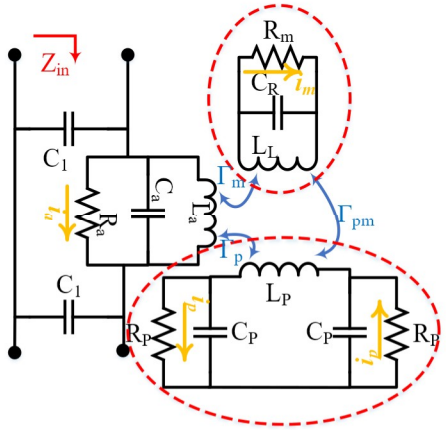

Figure 2. Equivalent circuit of single element.

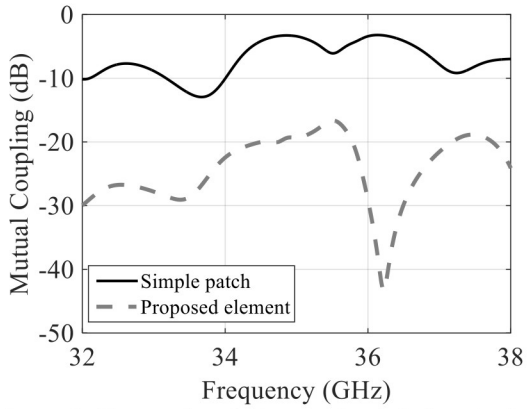

Figure 3. Comparison between simulated mutual coupling of proposed antenna with simple patch in 0.35λ0 distance

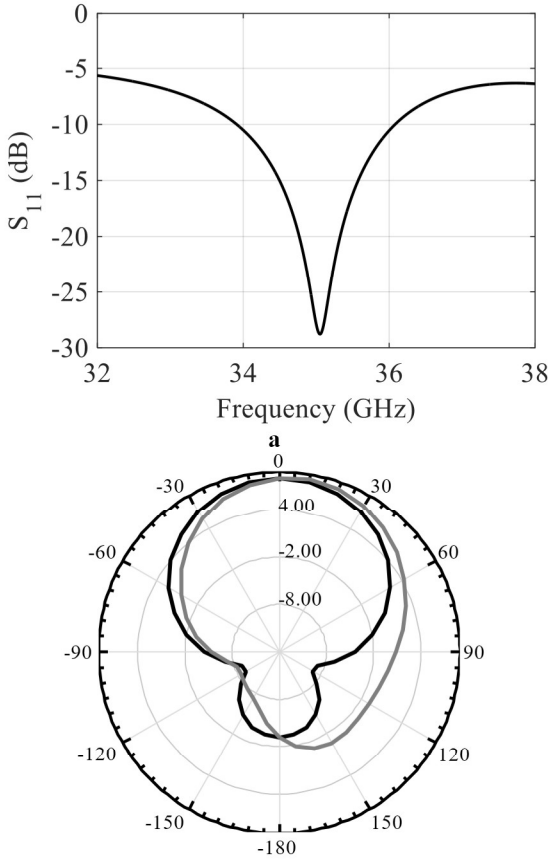

Figure 4. The simulated results of proposed antenna elements at a) S11 and b) pattern at 35GHz

3. Butler Matrix and Broad Band Phase Shifter

The proposed feed network incorporates a semi-interdigital phase shifter (Figure 5a) to facilitate broadband operation. The Butler matrix configuration is optimized using Agilent ADS and consists of a crossover, two branch line couplers, and two broadband 45° phase shifters fabricated on Rogers 3010 substrate (thickness: 0.25 mm). The feed network

resonates at the ZOR frequency to achieve broadside radiation patterns and high-gain beam steering. Simulation results for the Butler matrix (Figures 6b, 6c, 6d) confirm its ability to evenly divide signals at output ports with phase differences of 45°, 90°, 135°, and 180°. This enables precise beam steering at 35 GHz, with spacing of 0.35 between output ports. The proposed design overcomes typical Butler matrix challenges, including crossover size and broadband phase-shifting accuracy. The results of the proposed Butler Matrix is presented in Fig. 6b, c and d. As seen in Fig.6b, the proposed Butler matrix is capable of dividing the signal at the output ports when each input port is excited. As aforementioned, by designing all resonance of the feed network, the ZOR resonance can save the broadside pattern at 35GHz and this state with scrutiny of Fig. 6c is realized. The proposed Butler matrix includes four input ports and four output ports, and the distance between the output feeding lines is 0.35 λ0-35GHz (λ0-35GHz wavelength in free space at 35GHz). By selecting each input (of four ports) as a driving input, the Butler matrix delivers four output signals with equal amplitude (-6dB) and phase differences of 45°, 90°, 135°, and 180°, respectively. This can arrange beam steering at different broadside angles on a transverse plane perpendicular to the substrate (Figure.6d).

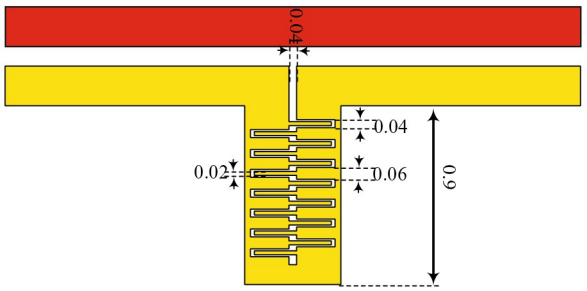

a

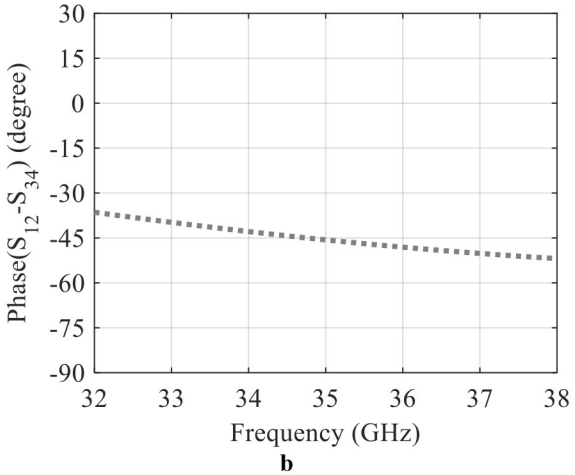

b

Figure 5. The structure and results of broadband 45° phase shifter. a) structure and b) phase shifting

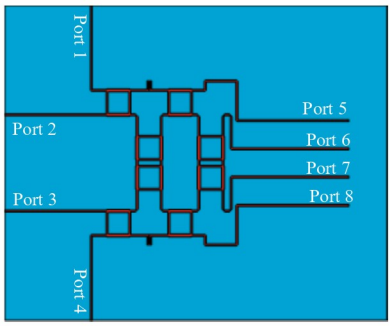

a

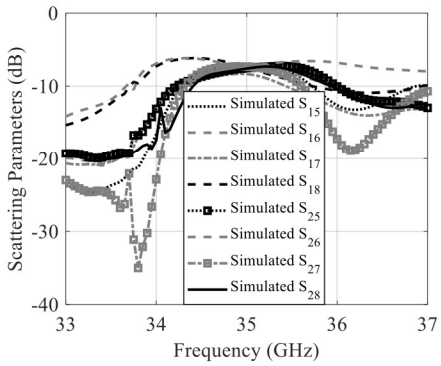

b

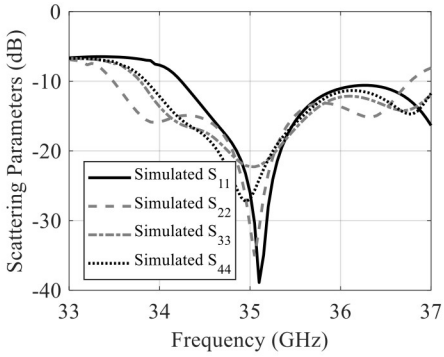

c

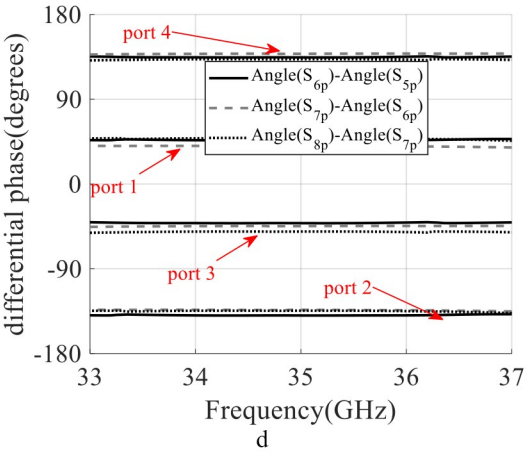

d

Figure 6. Configuration of Butler matrix feed network with broadband phase shifting a) configuration of proposed Butler matrix feed network, b) Insertion loss between inputs and outputs results, c) reflection coefficient of input ports, and d) phase shifting between output ports.

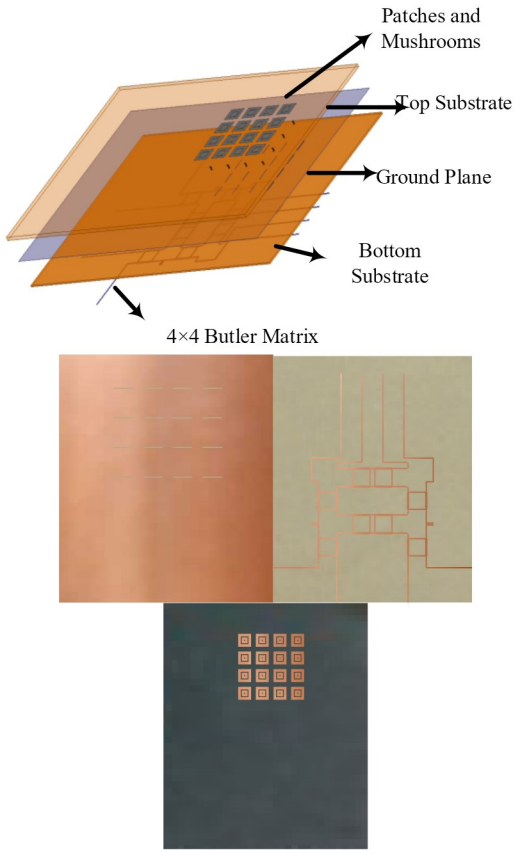

Figure 7. The configuration and sample of fabricated proposed beam steering antenna

4. Antenna results and discussion

Fabricated prototypes of the proposed beam-steering antenna were measured using an Agilent 8510XF vector network analyzer. Simulated and measured scattering parameters (Figure 8) demonstrate good agreement across the operating band (32.11–37.86 GHz). Beamforming states were validated through simulated 3D radiation patterns (Figure 9) and measured normalized patterns (Figure 10). Steered beams achieved gains of 17–21.9 dBi, highlighting the array's capability for high-gain applications.

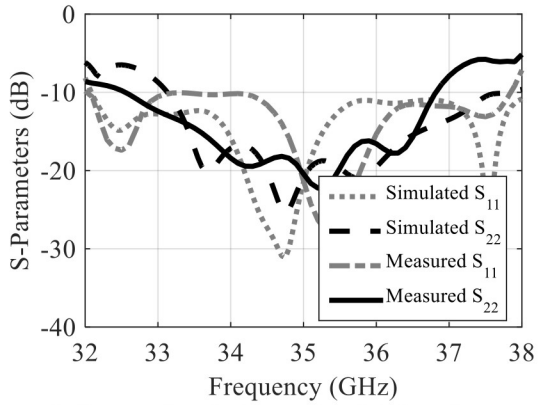

Figure 8. Comparison between simulated and measured results for S11 and S22

The 3D-simulated radiation pattern of the antenna at 35GHz for ports 1, 2, 3, and 4 is shown in Fig. 9. The normalized measured radiation pattern of the planar microstrip antenna array at 35 and 37 GHz with 4×4 elements with the proposed Butler matrix is displayed in Fig. 10. As the figure clearly shows, the pattern direction is variated by changing input ports. The beams were successfully steered from broadside with peak gains ranging from 17 to 21.9 dBi. In Table 1, the resulting gain is compared with similar previous works.

Table 2. Performances of the published FP antennas ([i] is this work)

Ref	Frq (GHz)	Height of air layer	Substrate layers/ antenna height	HPBW, %	Gain
[12]	.60	$\lambda_o/2$	3/0.52 λ_o	0.5	15.2
[13]	94	$\lambda_o/2$	Non-planar/1.02 λ_o	1	13
[14]	35	$\lambda_o/2$	3/0.67 λ_o	7.1	16.1
[15]	63	3 λ_o/10	2/0.52 λ_o	4.3	11
[16]	44	no	1/0.23 λ_o	1	14
[i]	35	no	3/0.25 λ_o	6.2	17.4

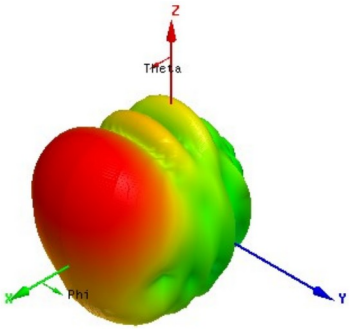

(a)

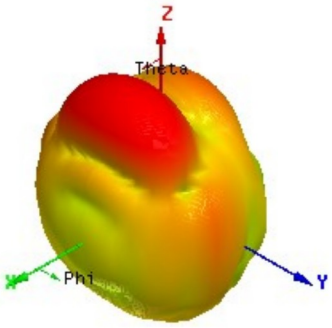

(b)

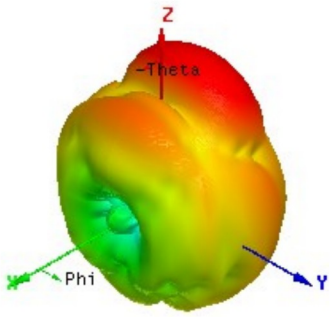

(c)

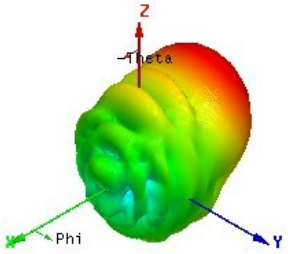

(d)

Figure 9. Simulated 3D patterns corresponding to ports 1–4 at 35 GHz: (a) port 1, (b) port 2, (c) port 3, and (d) port 4.

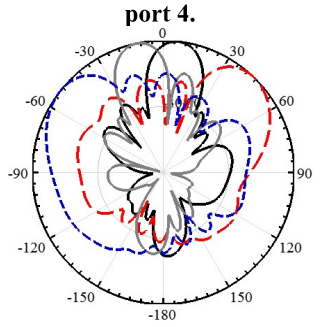

(a)

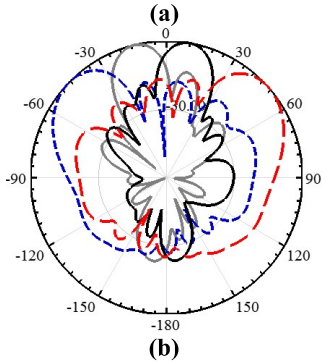

(b)

Figure 10. Normalized measured radiation pattern of the planar microstrip antenna array at 35 and 37 GHz with gains ranging from 17 to 21.9 dBi.

.

5. Conclusions

In this work, a beam steering array antenna that combines 4×4 radiated elements with low distance and mutual coupling between them in a compact size is introduced. The beam steering is realized using a 4×4 Butler matrix feed network. In order to solve phase delay problem between output ports, novel broadband 45° phase shifters that are optimized to achieve a compact size and wide bandwidth performance are used. The mentioned features are meant to provide a beam-steerable antenna with about 19dBi average gain in the desired impedance BWs. This antenna can be used in many applications such as 5G mobile and automotive radar applications.

References

[1] K. Buell, H. Mosallaei., and K. Sarabandi. “A substrate for small patch antennas providing tunable miniaturization factors,” IEEE Trans on Microwave Theory and Techniques, Vol. 51, no. 1, pp. 135_146, Jan. 2006.

[2] S.T.Ko and J.H.Lee, “Aperture coupled metamaterial patch antenna with broad E-plane beamwidth for millimeter wave application, ” IEEE Antennas and Propagation Society International Symposium (APSURSI) , pp. 1796_1797, Jul. 2013.

[3] C.H.Lee and J.H.Lee, “Millimeter-wave wide beamwidth aperture–coupled antenna designed by mode synthesis, ”M icrowave and Optical Technology Letters, Vol.57 ,pp. 1255_1259,May.2015.

[4] S. T. Ko and J. H. Lee, “Hybrid Zeroth-Order Resonance Patch Antenna with Broad E-Plane Beamwidth, ” IEEE Trans on Antennas and Propagation, vol. 61, no. 1, pp. 19_25, Jan. 2013.

[5] A.Artemenko, A.Mozharovskiy, A.Maltsev, R. Maslennikov, A. Sevastyanov and V. Ssorin, “Experimental Characterization of E-Band Two-Dimensional Electronically Beam-Steerable Integrated Lens Antennas, ” IEEE Antennas and Wireless Propagation Letters, vol. 12, pp. 1188_1191, 2013.

[6] Donelli, M., Febvre, P., "An inexpensive reconfigurable planar array for Wi-Fi applications ," Progress In Electromagnetics Research C Volume 28, 2012, Pages 71-81.

[7] F. Robol, M. Donelli, "Circularly polarized monopole hook antenna for ISM-band systems" in Microwave and optical technology letters, v. 60, n. 6 (2018).

[8] T. Moriyama, M. Manekiya, M. Donelli "A compact switched-beam planar antenna array for wireless sensors operating at Wi-Fi band" Progress In Electromagnetics Research C, Volume 83, 2018, Pages 137-145.

[9] A.Bakhtiari,R.A.Sadeghzadeh and M. Naser. Moghadasi ,"Gain Enhanced Miniaturized Microstrip Patch Antenna Using Metamaterial Superstrates,"IETE Journal of Research,pp.1-6, 2018.

[10] A.Bakhtiari,R.A.Sadeghzadeh and M. Naser. Moghadasi . “Millimeter-Wave Beam-Steering High Gain Array Antenna by Utilizing Metamaterial Zeroth-Order Resonance Elements and Fabry-Perot Technique.” International Journal of Microwave and Wireless Technologies, vol. 10, no. 3, pp. 376–382, 2018.

[11] J.R.James, P. S Hall, “Handbook of Microstrip Antennas”, Volume 1&2' (Electromagnetic Waves, 1989); IET Digital Library.

[12] Geng C, Lian JW, Guo YJ, Ding D. Millimeter-Wave Three-Layer Substrate-Integrated 9×9 Butler Matrix and Its Application to Wide-Angle Endfire Multibeam Metasurface Antenna. IEEE Transactions on Microwave Theory and Techniques. 2024 Feb 28.

[13] Vallappil, Arshad Karimbu, et al. "Compact Metamaterial Based $4\times4 $ Butler Matrix With Improved Bandwidth for 5G Applications." IEEE Access 8 (2020): 13573-13583.